

SIMPLE METHOD OF DYNAMIC DISPLACEMENT RECORD OF CONTACTS DRIVEN BY INDUCTIVE DYNAMIC DRIVE

Piotr Jankowski, Bolesław Dudojć, Janusz Mindykowski

*Gdynia maritime University, Electrical Faculty' Department of Marine Electrical Power Engineering, Morska 81-87, 81-225 Gdynia, Poland
(✉ boldu@am.gdynia.pl, +48 58 690 1390, keopiotr@am.gdynia.pl, janmind@am.gdynia.pl)*

Abstract

Inductive dynamic drive is the main part of ultra-fast hybrid breakers. Its principle of work is based on the Thomson phenomenon, where a coil is powered by pulse current (most often from a bank of capacitors) and whose field induces eddy currents in the coupled disc. As a result the disc is impacted by a significant force causing its movement. In the paper the authors present research results of a new simple optimeter used for recording of ultra-fast displacements of an inductive dynamic drive disk. The presented solution is characterized by very simple construction, a high output signal and relatively good linearity.

© 2009 Polish Academy of Sciences. All rights reserved

1. Introduction

Higher and higher requirements imposed on protective-distributive equipment in electrical power engineering have caused the development of ultra-fast hybrid breakers (HB) (Figs 1 and 2) [1]. The tendency and the ultimate aim is to have a short-circuit release characterized, first of all, by a very short operation time and repeatability. The period during which in this kind of circuit breaker, the short-circuit is completely broken lasts less than 1ms. The construction of the HB presented in Fig. 1 allows to switch the short-circuit off without the electric arc. Such requirements have resulted in an increase of interest in drives that cause fast movement of contacts. The most important features that a drive should possess are: the ability to reach very high accelerations, the stability of mechanical characteristics and the long-lasting reliability. Among the drives that satisfy the above conditions, the inductive-dynamic drives (IDD) are most frequently made use of.

The new concept of an optimeter designed to record ultra-fast displacement was presented at the TC 4 IMEKO 2008 Symposium and IWADC Workshop in the work of the authors [2]. This work is an extension of that paper.

The main parts of the inductive dynamic drive (Fig. 3) are: one-layer coil of small inductiveness, a bank of capacitors of minimum loss and a well-conducting part (called

a disc or a ring), which is coupled inductively with the coil. The principle of work of an IDD is based on creating a pulse magnetic field powered by a coil from a bank of capacitors. The pulse magnetic field induces eddy currents in the disc, therefore the Lorentz force appears as a result of electromagnetic impact. The above phenomenon above is often called the Thomson effect after the name of scientist who discovered it. Drives based on this effect are called inductive dynamic as opposed to a classic two-coil inductive drive. There exists an electrodynamic IDD model based on the results of equation (1) with appropriate starting and edge conditions.

$$\frac{\partial \mathbf{B}}{\partial t} = \frac{1}{\mu \cdot \gamma} \nabla^2 \mathbf{B} + \nabla \times (\mathbf{v} \times \mathbf{B}), \tag{1}$$

where μ – magnetic permittivity, γ – conductance.

Taking into consideration the cylindric symmetry of the considered system and linearity of environment, equation (1) should be solved in a system together with an equation of coil power supply circuit and an equation of disc movement.

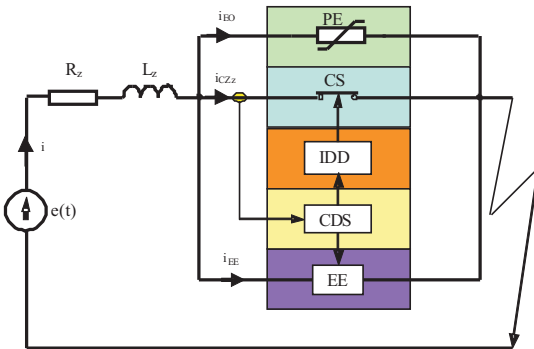


Fig. 1. Scheme of HB in short-circuit.

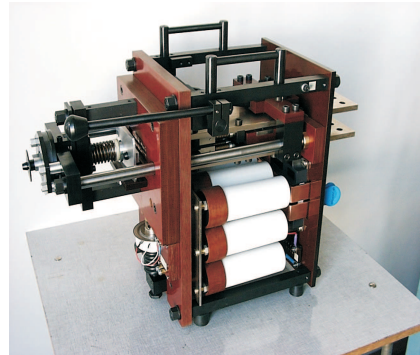


Fig. 2. Physical model of ultra-rapid HB [1].

CS– contact segment, IDD - inductive dynamic drive,
 EE – power electronics element, PE– protective element,
 CDS - system of current detection.

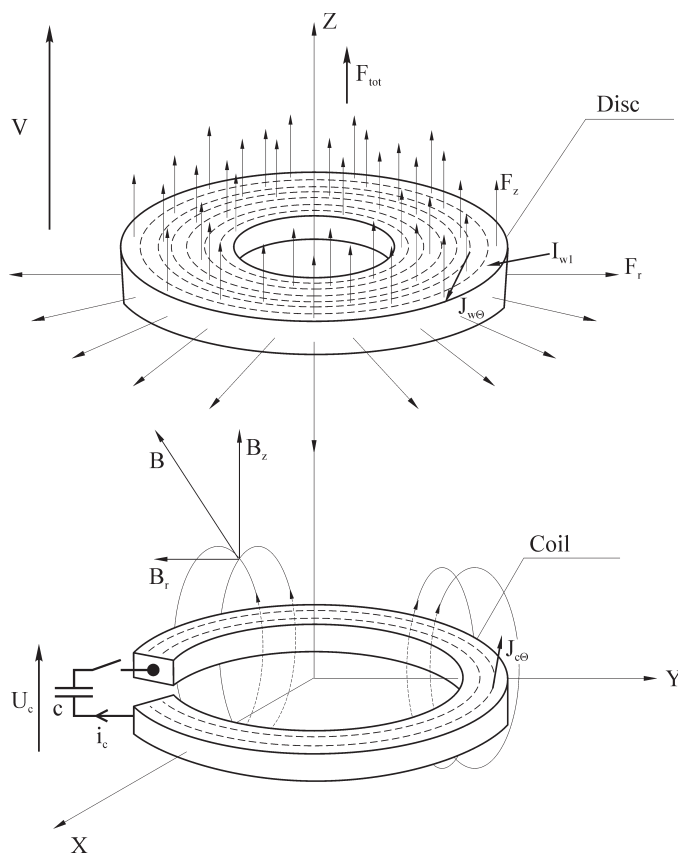


Fig. 3. IDD-System of coaxial inductor (coil) and disc.

The realization of such a circuit-field model was described in detail in papers [3] and [4]. This model assumes numerous simplifications, from which the stiffness of the secondary part of the disc is the most important. This assumption is true only while choosing a disc of relevant size with regard to the produced force. The described effect is able to make permanent changes in the conductive part and can be used even to form sheets.

2. Simulation results

Despite of simplifications, simulation research with the use of electrodynamic model makes it possible to describe general directions while choosing the drive parameters.

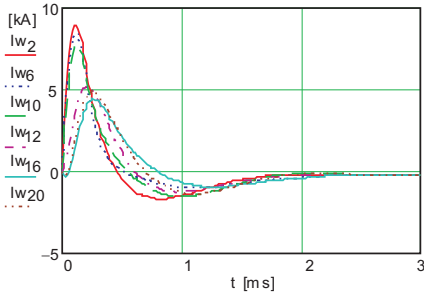


Fig. 4. Disc currents in few filaments (Fig.3).

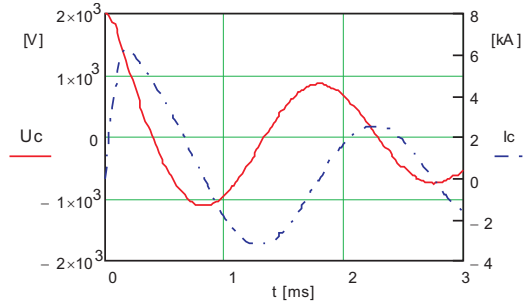


Fig. 5. Capacitor voltage and coil current (Fig.3).

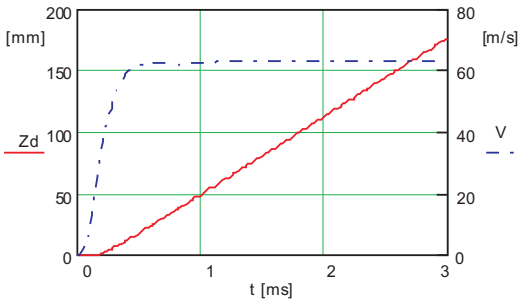


Fig. 6. Displacement and velocity of disc.

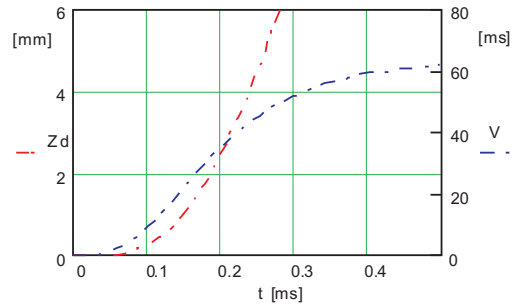


Fig. 7. Enlargement of box for Fig.6.

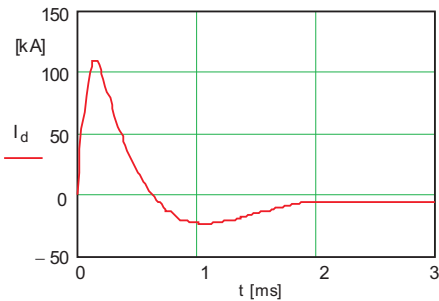


Fig. 8. Entire current of disc.

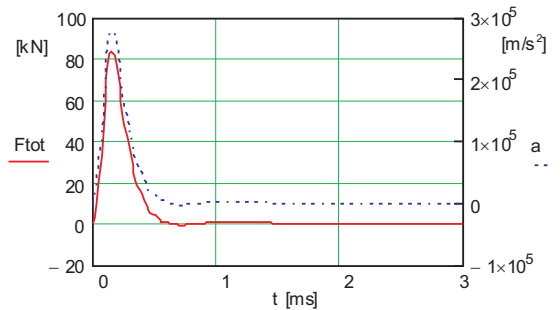


Fig. 9. Resultant force and acceleration.

In order to illustrate which values can reach certain figures in IDD, simulations were carried out with the use of a program realizing the model above for parameters from Table 1 with use of great initial energy of the bank of capacitors ($W=2$ kJ) (Fig. 4-9). Fig. 4 shows eddy currents in some selected disc layers. It is obvious that the distribution of the magnetic field, and therefore the density of current along disc thickness is strongly damped. It means that the total disc current of maximum magnitude more than 100 kA (Fig. 8) flows mainly in the surface layer of the disc, the closest one to the coil. In spite of the temporary character of the short-time phenomenon, such big current values can have an influence on the resistance of the conducting material. This fact would require considering thermodynamic phenomena in the model, as research in [3] showed a strong influence of both the material's resistance and the coil circuit on the obtained values of the researched parameters. In Fig. 6 there are presented displacements z_d (left axis) and speed v (right axis) of the disc.

However, as the gap that needs to be obtained by the breakers' contacts does not exceed 4 mm, a large picture of a window from Fig. 6 was presented in Fig. 7. This picture indicates that the disc can reach the required distance in a time less than 250 μ s. Fig. 9 presents the resultant force F_{tot} impacting the disc (left axis) and acceleration a of the disc weighing 0.3 kg (right axis). It is worth to underline that such a great acceleration can be obtained at a relevant size of the disc, minimizing its mass with possibly maximum force. Most often they are contradictory conditions and exceeding a certain balance between force and mass will lead to disc vibrations in the best case. In an extreme case, while further decreasing the thickness of the conducting surface it can become permanently deformed. There is a well-known method of forming metal covers with the use of the Thomson effect [5], [6]. As it is shown in the above simulations in extreme conditions, a complete model should take into account not only electrodynamic phenomena but magnetoelasticity [4] and thermodynamic ones as well. The problem above is also part of a coupled phenomena area. Hence, experiments are still a very important part of research and design of IDD. In the experimental examinations of this type of drives it is necessary to apply a device of appropriate quality which registers any displacement of the IDD disk [3]. A meter used to measure the disk displacement should possess the following features: small mass of a mobile element, immunity to the external magnetic field, lack of friction of the meter elements, resistance to vibration, endurance to the forces occurring during the displacements and lack of inertia. Additionally, the meter should be characterized by high dynamics, because it measures the displacements at ultra-fast instantaneous accelerations reaching even more than $2 \cdot 10^5$ g (g-Earth gravity) as it could have been observed in Fig. 9. The existing manufactured meters, designed to measure displacements, such as: resistance potentiometers, inductive or capacitive transducers, do not satisfy the requirements that would allow these devices to measure such dynamic displacements. There exist laboratory optical solutions, which most often do not make a direct measurement, however the signal must be transformed (most often through additional modules). An optical measurement system used for measurement of displacement of formed sheets

seems an interesting solution. This solution is based on transmission of light reflected by an optic fibre from a moving surface to an optical sensor. Lack of measurement contact and lack of loading the moving part with additional mass is an advantage of this system. However, its disadvantage lack of linearity of static characteristics and need of calculating it for other types of sheets.

Therefore, a necessity has arisen to construct an optimizer enabling the registration of element movement but which at the same time does not have the drawbacks of the traditional meters.

3. The construction of an optimizer designed to measure

The main measuring element of the meter is a photosensitive element consisting of photoelements connected in parallel, which constitute a “photosensitive ruler” (Fig.10).

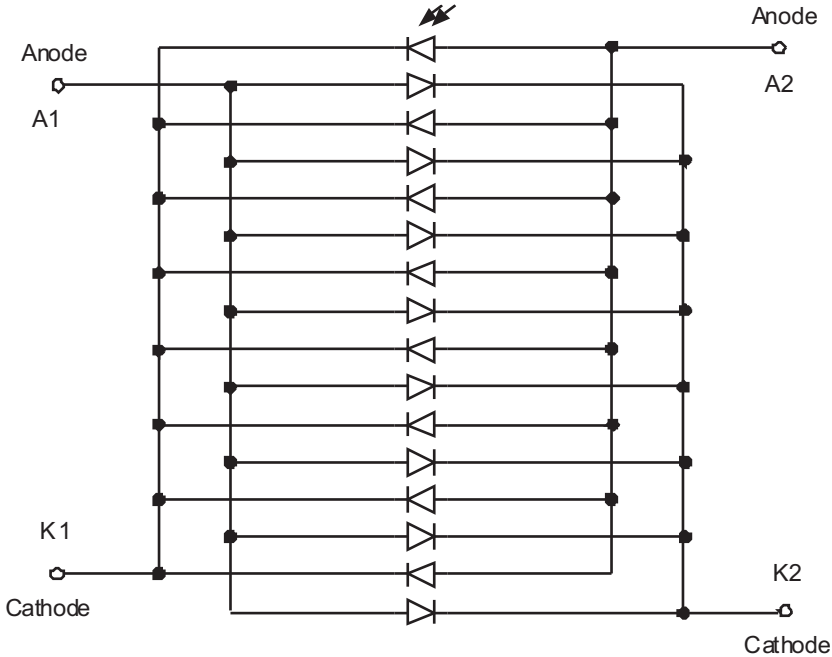


Fig. 10. Photosensitive ruler- photoelements connected in parallel.

The “photosensitive ruler” (photoelement) is situated under an aluminum diaphragm in Fig. 11. The diaphragm is connected to the IDD disc by a light aluminum pull rod.

During the movement of the disc, the displacing diaphragm uncovers the photosensitive element. An increase of the lit surface of the photoelement causes an increase in the output signal on its terminals.

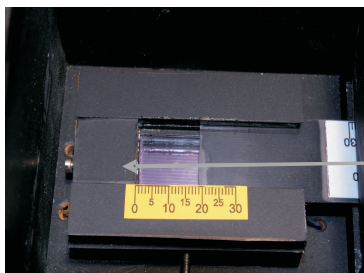


Fig. 11. The view of “a photosensitive ruler” with a diaphragm.

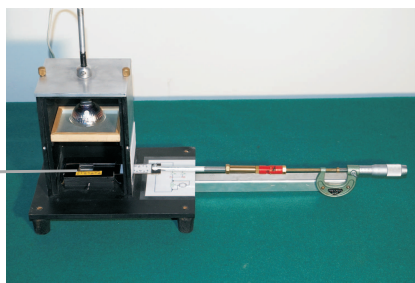


Fig. 12. The external view of an optimeter.

The meter is equipped with a glass filter made of clouded glass so as to improve the smoothness of visible radiation distribution on the whole surface of this photoelement. The case of the optimeter is made of aluminum and is covered from the inside with flattening black paint so as to prevent possible light reflections and refractions and to minimize the influence of the external light getting out through a slot in the case. The view of the optimeter, in which the diaphragm is connected with a micrometric gauge for calibration, is presented in Fig. 12. The measurement system construction which records the displacement is presented in Fig. 13.

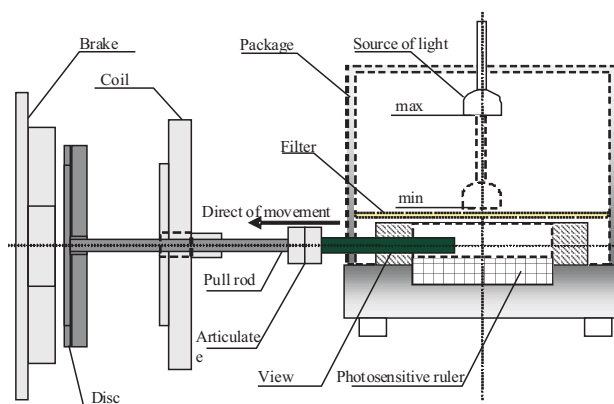


Fig. 13. Construction of the measuring system of displacement.

4. Research of the static characteristics of the optimeter

The photoelement was examined in two systems: a system of a photo-voltaic cell and a system of a photo-diode supplied from an external voltage source.

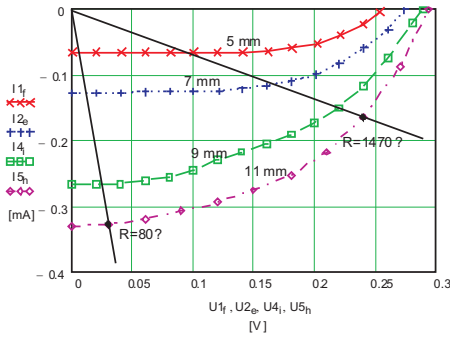


Fig. 14. The current-voltage characteristics of the photo-voltaic cell.

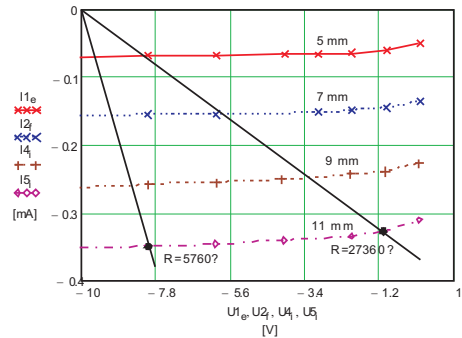


Fig. 15. The photo-diode characteristics.

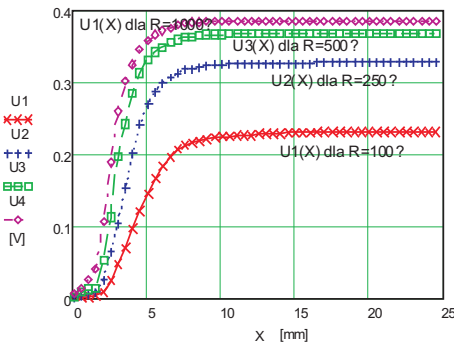


Fig. 16. The characteristics of the voltage in the displacement function $U=f(X)$ for a lamp of 20W for $R=var$.

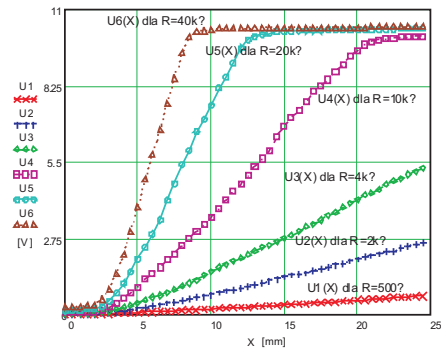


Fig. 17. The characteristics of the voltage in the displacement function $U=f(X)$ for a lamp of 3.2W at different loads.

While carrying out research of the optimizer the focus was put on finding the optimal static characteristics. The two most important parameters characterizing the meter which were analyzed were: sensitivity and linearity. The sensitivity measured in the examinations was defined as the ratio of the voltage increment to the displacement increment ($\Delta v/\Delta x$). Sensitivity may have a great influence on measurements errors, because the IDD disc moves within a distances of about 30 mm, but the fundamental displacement essential for a hybrid breaker to operate does not exceed 5 mm.

In the first stage the current-voltage characteristics were measured for a few initial positions of the diaphragm and for different sources of light. This made it possible to determine preliminarily a range of the load resistance, which provides the best working conditions with regard to both: linearity and sensitivity of the examined optimizer. Fig. 14 presents the exemplary family of the current-voltage characteristics in the system of the photo-voltaic cell, whereas Fig. 15 presents it in the system of the photo-diode for 3.5W halogen light.

During the research the influence of a position of the glass filter situated a different heights above the photoelement inside the meter was checked. It was noticed that the distance from the filter to the lamp does not have any significant influence on the characteristics. Additionally, four other light sources lighting the photosensitive element were examined. Among them were: the halogen lamps with a power of 50, 20, 3.5 W and a 14 W fluorescent lamp with electric power corresponding (according to the manufacturer) to 70 W of incandescent lighting.

The measurements range in the system with a photo-voltaic cell can be extended by reducing the load resistance. Exemplary characteristics for the same light source at different load resistances of the photovoltaic cell system are presented in Fig. 16. Fig. 17 presents a family of the characteristics of the examined optimizer in the photo-diode system for various R for a 3.5 W the halogen lamp. This time, the characteristics for $R=40\text{ k}\Omega$ obtain highest sensitivity in comparison with the characteristics for a 50 W bulb with the load equal to $500\ \Omega$. Simultaneously, this characteristics in the range up to 8mm has better linearity than in case of the light of higher power.

On the basis of the investigations carried out it was noticed that the operation of the “photo-sensitive element ruler” in the system of the photo-voltaic cell does not guarantee the appropriate measurement range because of the quick saturation of the characteristics with simultaneously smaller sensitivity than the characteristics in the system of the photo-diode. In both cases the photoelement of the examined meter was characterized by the initial phase of insensibility.

Among the characteristics measured in the photo-diode system the biggest sensitivity was demonstrated by the characteristics for the halogen light source of 50 W. Yet, the use of such a powerful bulb caused excessive heating of the whole meter, which additionally affects the measurement results. Therefore, the system with the halogen bulb of 3.5 W at the load of $40\text{ k}\Omega$ was again selected from all the other light sources, which constituted a compromise between the highest sensitivity and linearity.

The little power of the bulb ensured fast thermal stability from the very start. With regard to the phase of non-sensitivity, the part of the selected characteristics in the range from 3 to 8 mm was taken into account to register small displacements. If the necessity to register bigger displacements appeared, it would be necessary to reduce the circuit resistance in relation to the required range.

5. Measurements of the ultra-fast displacements

The measurement system designed to register displacements of the disk and the coil current is presented in Fig. 19 and its physical realization in Fig. 18. Parameters of the researched inductive dynamic drive are presented in Table 1. The voltage oscillogram obtained from the meter for $R=40\text{ k}\Omega$ is shown in Fig. 20.

Table 1. Selected data of the IDD.

Outer radius of disc: $R_z=7$ cm	Inner radius of disc: $R_w=4.5$ cm	Add mass: 0.2 kg	Material of disc: duralumin Thickness of disc: $h=6$ mm	Initial energy of capacitor: $W=50$ J, 500 J, 2 kJ
Outer radius of coil: $r_z=7$ cm	Inner radius of coil: $r_w=4.5$ cm	Winding of coil $z_w=24$	Thickness of coil: $h_c=1$ cm	Capacitance of capacitor: $C=1000$ μ F

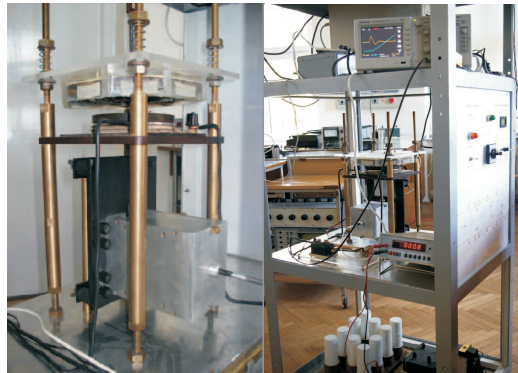


Fig. 18. The optimizer connected with IDD and the measuring system.

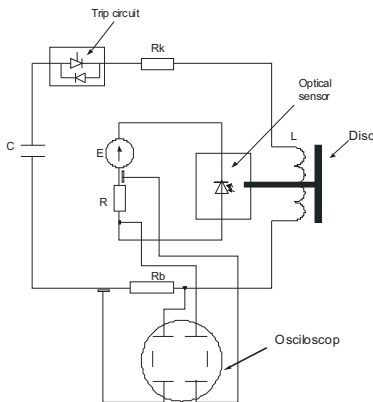


Fig. 19. The measurement system to examine the coil current and the disc displacement.

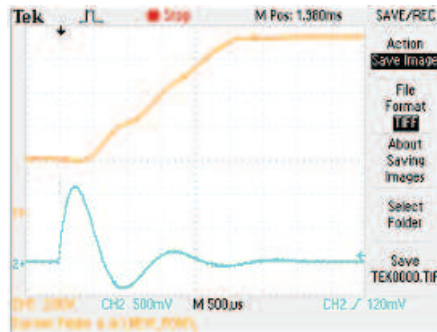


Fig. 20. The oscillogram of the disc displacement and the coil current.

Because the whole characteristics of the photoelectric meter is not linear and the output result is the voltage in a function of time $U=f(t)$, it is necessary to perform conversion of the characteristics in order to obtain the variation of displacement in the

time function $x=f(t)$. The process of changing the scale was performed by the program realized in a Mathcad environment.

In order to check the correctness of system operation, the characteristic obtained from the examined optimeter was compared with the characteristics of movement obtained from a brand-new Megatrom potentiometer (Fig. 22). The characteristics registered by the optimeter and potentiometer entered into Mathcad before the conversion are presented in Figs 21 and 23. On the other hand, the comparison of the characteristics of the displacement variation in the time function after the conversion and approximation processing obtained from both meters is presented in Fig. 24.

The biggest relative difference occurring in the initial phase of movement between the characteristics obtained from the optimeter and the potentiometer did not exceed 3.5%.

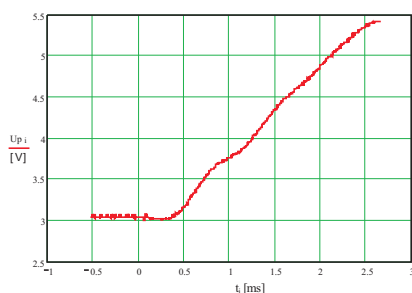


Fig. 21. The $U(t)$ characteristics of potentiometer.



Fig. 22. The Megatrom Company potentiometer

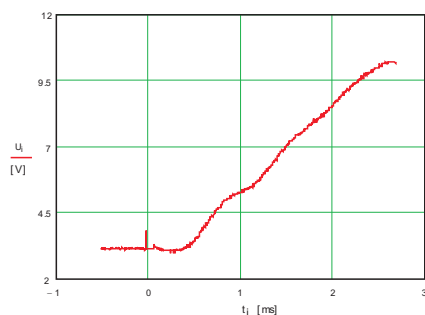


Fig. 23. The $U(t)$ characteristic of optimeter.

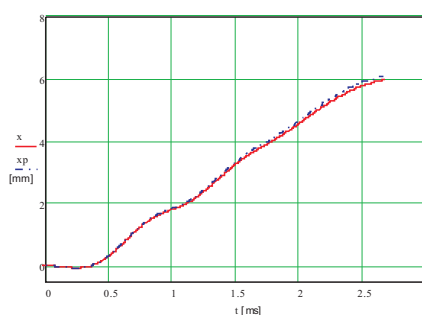


Fig. 24. The comparison of the obtained characteristics from the optimeter (x) and the potentiometer (x_p).

6. Method of measurement of last testing distance

Verification of the optimeter properties by comparison with a resistance sensor was carried out for a small energy. Further increase of voltage of a bank of capacitors caused a loss of connection in a resistance sensor, due to which the measurement was not precise.

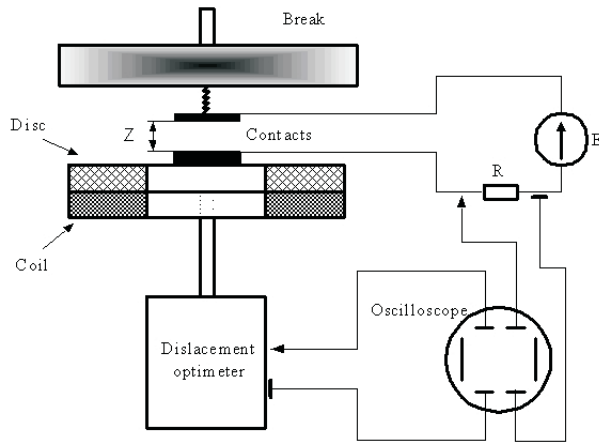


Fig. 25. System for registration of time when the set displacement is executed.

As it is expected to eventually carry out measurement at energies up to 2 kJ, there has been a trial of verifying the constructed optical sensor at the highest initial voltage of a bank of capacitors. Verification was based on determining one point of characteristics at one shot. The measurement system used for this purpose has been presented in Fig. 25. The measurement was based on setting connecting contacts closing an inertialess circuit at a certain distance. In the same experiment displacement characteristics were measured. Leap of voltage in a inertialess circuit was indicated as a point with coordinates (z, t) , which was compared with a point with the same coordinates on the characteristic of the optimeter.

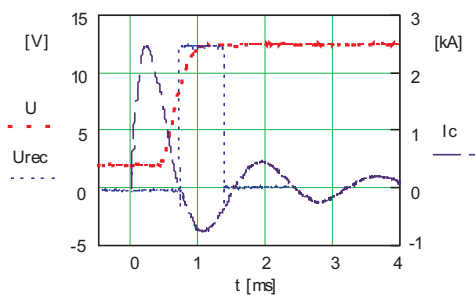


Fig.26. Impulse showing the moment of last testing distance.

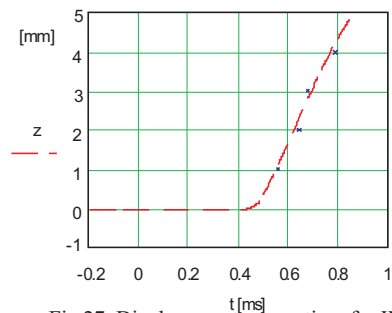


Fig.27. Displacement versus time for $W=245J$.

In Fig. 26 there are presented curves of coil current and of disc displacement registered by the optimizer and a voltage step indicating the moment of closing of connecting contacts (Fig. 25). Fig. 27 shows the curve of displacement after conversion and, in its background, the points registered in the system in Fig. 25 for gap of connecting contacts $z=1$ mm, 2 mm, 3 mm, 4 mm. The relative difference did not exceed 4% in any of the cases, which confirms proper work of the optimizer at higher energy of the bank.

It is worth to emphasize that for each shot (for $U_c=700$ V) the displacement characteristics were the same, which confirmed the system repeatability.

7. Conclusions

One has to emphasize that the presented optimizer will be employed to register the much greater dynamic displacement than the one shown in Fig. 27. To ensure the correct operation of HB, the IDD must displace the contacts within about 100 μ s to a distance of 1 mm. Therefore the research into the inductive dynamic drive in the range of 5 mm of displacement is fully satisfactory.

It seems, therefore, that the presented optimizer allows recording the movement of objects obtaining a displacement variation up to 20 mm in a short time, under the short duration pulse force. The range of the maximal speed is more limited because of the mechanical endurance of the drive disk rather than because of the operation frequency of the photoelement, which does not exceed 100 MHz. The optimizer is screened against the influence of the magnetic field generated by the drive coil. Simultaneously, it is characterized by simplicity of construction, which does not require any additional complex systems [7], [8], [9].

References

- [1] J. Czucha, J. Woloszyn, M. Woloszyn: "The comparison of ultra fast A.C. hybrid circuit breakers with GTO and IGBT". *35th Universities Power Engineering Conference UPEC'2000*, Belfast, 6-8 September 2000.
- [2] P. Jankowski, B. Dudojć, J. Mindykowski: "An optimizer designed to register ultra fast displacement". *TC4 IMEKO 2008 Symposium and IWADC*, Florence, Italy, September 2008, Proceedings, CD-ROM.
- [3] P. Jankowski, K. Jakubiuk: "Model obwodowy napędu indukcyjno-dynamicznego". *XIX Seminarium z Podstaw Elektrotechniki i Teorii obwodów*, Gliwice – Ustroń 1996. pp. 243–246. (in Polish).
- [4] P. Jankowski, S. Rymkiewicz: "Stress analysis of magnetoelastically vibrating disc". *ACTA TECHNICA CSAV Academy of Sciences of the Czech Republic*, Praha 2008.
- [5] J. Bednarczyk: *Electrodynamic metal forming*, Editor AGH Krakow, 2007.(in Polish).
- [6] W. Stiepanow: *Impulsnaja metaloobrabotka w sudowom maszynostrojenii*. L., Sudostrojenije, 1968.

- [7] J. Bednarczyk, G. Głuch, E. Wojnar, T. Załuski: "Using an Optical Fibre Sensor to Measure Displacement of Electrodynamically Formed Sheet Metal". *Metrology and Measurement Systems*, vol. XIV 3/2007, pp. 437–452.
- [8] V.V. Kulagin: "Optical displacement transducer with pulsed pump for experiments with probe bodies". *Journal of Optics B: Quantum and Semiclassical Optics*, vol. 2, no. 2, 2000, pp. 100–104(5).
- [9] D. Perla, R. Gaudino, G. Perrone, S. Abrate: *Optical displacement transducer, displacement measurement system and method for displacement detection there from*, US Patent (No:7323678) Issued on January 29, 2008.